Leukocyte Antigen-related Protein Tyrosine Phosphatase Negatively Regulates Hydrogen Peroxide-induced Vascular Smooth Muscle Cell Apoptosis[*]

Juxiang Li, Xi-Lin Niu, and Nageswara R. Madamanchi[1]

From the Department of Medicine, Carolina Cardiovascular Biology Center, University of North Carolina, Chapel Hill, North Carolina 27599-7126

Reactive oxygen species (ROS) have been implicated in vascular smooth muscle cell (VSMC) apoptosis, a hallmark of advanced atherosclerotic lesions. Transient oxidation and inactivation of protein-tyrosine phosphatases play a critical role in cellular response to ROS production. However, the function of leukocyte antigen-related (LAR) protein-tyrosine phosphatase in ROS signaling is not known. To determine the expression of LAR in ROS-induced apoptosis, we investigated hydrogen peroxide-induced cell death and signaling in aortic VSMCs from wild-type and LAR$^{-/-}$ mice. Histone-associated DNA fragmentation and caspase-3/7 activity were significantly enhanced, mitochondrial membrane integrity was compromised, and cell viability was significantly decreased following H$_2$O$_2$ treatment in LAR$^{-/-}$ VSMCs compared with wild-type cells. Stronger and sustained increase in autophosphorylation and activity of Fyn, an Src family tyrosine kinase, was observed in LAR$^{-/-}$ cells compared with wild-type cells following H$_2$O$_2$ treatment. LAR binds to activated Fyn in H$_2$O$_2$-treated VSMCs, and recombinant LAR dephosphorylates phosphorylated-Fyn *in vitro*. In addition, LAR deficiency enhanced H$_2$O$_2$-induced phosphorylation of Janus kinase 2 (JAK2), signal transducer and activator of transcription 3 (STAT3), and p38 mitogen-activated protein kinase (MAPK). PP2, a Fyn-specific inhibitor, blocked JAK2, STAT3, and p38 MAPK activation and significantly attenuated apoptosis induced by H$_2$O$_2$. AG490, a JAK2-specific inhibitor, significantly attenuated H$_2$O$_2$-induced apoptosis, and blocked H$_2$O$_2$-induced activation of STAT3, but not p38 MAPK in both wild-type and LAR$^{-/-}$ VSMCs. Attenuation of Fyn expression by short hairpin RNA significantly decreased H$_2$O$_2$-induced downstream signaling and apoptosis in VSMCs. Together, these data indicate that LAR regulates Fyn/JAK2/STAT3 and Fyn/p38 MAPK pathways involved in ROS-induced apoptosis.

Apoptosis is an essential component of normal development as well as of most developmental abnormalities and human diseases (1). Vascular smooth muscle cell (VSMC)[2] apoptosis occurs after vessel injury, in remodeling, and in advanced atherosclerotic lesions (2–4). A significant increase in VSMC death rate was observed in unstable *versus* stable angina plaques, suggesting the involvement of VSMC apoptosis in plaque rupture (5). Indeed, direct stimulation of VSMC apoptosis induces destabilization and rupture of atherosclerotic plaques (6, 7). Plaque rupture often leads to thrombosis with clinical manifestations of myocardial infarction or stroke. Atherosclerotic lesions are a highly pro-oxidant environment and contain high levels of reactive oxygen species (ROS), which can induce VSMC apoptosis (8–11).

In addition to atherosclerosis, ROS have been implicated in hypertension and other vascular diseases, and intracellular signaling cascades stimulated by ROS play an important role in the pathogenesis of these diseases. ROS-induced stimulation of protein phosphorylation pathways modulates transcription factor activities and gene expression, which results in a variety of responses such as cell growth, differentiation, or apoptosis (12, 13). The particular response observed will depend on the cell type, and the concentration and duration of ROS production.

Hydrogen peroxide, the most stable form of ROS, inhibits protein-tyrosine phosphatases (PTPs) *in vitro* and reversibly in intact cells (14–17). PTPs contain a catalytically essential cysteine residue in their signature active site motif, HCXXGXXR(S/T) (where X is any amino acid), with an extremely low pK_a (18). The low pK_a promotes the function of the cysteine as a nucleophile in catalysis but renders it a target of oxidation with concomitant inhibition of PTP activity (14, 19). Recently, Groen *et al.* (20) reported that PTPs undergo differential oxidation at physiological pH and H$_2$O$_2$ concentrations, which indicates that cellular responses are fine-tuned to various oxidative stimuli. ROS generation is the proximal event in cell surface receptor activation by growth factors and cytokines. PTPs control protein-tyrosine phosphorylation, which is a key regulatory mechanism of many intracellular signaling

---

[1] To whom correspondence should be addressed: 7312B Medical Biomolecular Research Bldg., University of North Carolina, Chapel Hill, NC 27599-7126. Tel.: 919-843-4584; Fax: 919-966-1012; E-mail: nrmadama@med.unc.edu.

[2] The abbreviations used are: VSMC, vascular smooth muscle cell; PP2, 4-amino-5-(4-chlorophenyl)-7-(t-butyl) pyrazolo[3,4-d] pyrimidine; ROS, reactive oxygen species; PTP, protein tyrosine phosphatase; JAK2, Janus kinase 2; STAT3, signal transducer and activator of transcription 3; MAPK, mitogen-activated protein kinase; FBS, fetal bovine serum; DMEM, Dulbecco's modified Eagle's medium; shRNA, short hairpin RNA; LAR, leukocyte antigen-related; ERK, extracellular signal-regulated kinase; MOPS, 4-morpholinepropanesulfonic acid; AdLAR, adenovirus-encoding LAR; CMV, cytomegalovirus; ANOVA, analysis of variance; SH2, Src homology 2.

pathways. Therefore, oxidation and inhibition of PTPs by ROS may be an initial and critical step for ROS and growth factor-induced signaling in cells (14, 21–23). However, very little is known about the role of individual PTPs in regulating ROS-induced signaling.

The mammalian leukocyte common antigen-related receptor (LAR) PTP family includes LAR, PTPδ, and PTPσ (24). LAR is expressed on the cell surface as a complex of two noncovalently associated subunits of 150 and 80 kDa, which are derived by the action of an endogenous protease on a preprotein (25, 26). The 150-kDa extracellular subunit comprises the N terminus of the protein, contains three tandem immunoglobulin-like domains and eight fibronectin-III like domains, and is modified by *N*-linked glycosylation. The 85-kDa C-terminal subunit contains a short ectodomain, a transmembrane domain, and two tandem phosphatase domains: the membrane-proximal D1 domain has phosphatase activity and the distal D2 domain is catalytically inactive but may regulate substrate specificity (27).

LAR has wide tissue distribution, including the lung, heart, brain, liver, and kidney, and it is expressed in various cell lineages, including epithelial cells, smooth muscle cells, and cardiomyocytes (25, 28). Cell culture and animal model studies have shown that this PTP acts as a negative regulator of insulin signaling (29–31). Recently, we reported that LAR regulates insulin-like growth factor-1 receptor signaling in VSMCs, and dysregulation of this PTP affects vascular pathophysiology (32).

In the present study, we examined the effect of LAR on H$_2$O$_2$-induced signal transduction pathways and apoptosis using aortic VSMCs derived from LAR knockout mice. Our results indicate that LAR regulates the viability of VSMCs under oxidative stress conditions. Absence of LAR enhances H$_2$O$_2$-induced VSMC apoptosis, by allowing hyperactivation of the Fyn/JAK2/STAT3 and Fyn/p38 MAPK pathways.

EXPERIMENTAL PROCEDURES

Materials—AG490, PP2, and H$_2$O$_2$ were purchased from Calbiochem. A MitoCapture^{TM} mitochondrial apoptosis detection kit was from BioVision. LAR enzyme was obtained from New England Biolabs. Two distinct anti-LAR antibodies, anti-LAR monoclonal (Cat. No. 610350, BD Transduction Laboratories) and goat anti-LAR polyclonal (sc-1119, Santa Cruz Biotechnology, Santa Cruz, CA), were used in this study. The monoclonal antibody, raised against an epitope corresponding to amino acids 24–194 of human LAR, recognizes 150-kDa extracellular segment, whereas goat polyclonal antibody, raised against an epitope in the C-terminal cytoplasmic domain of rat LAR, recognizes the 85-kDa C-terminal subunit. The other antibodies used were as follows: anti-Src (Tyr-416), anti-Src (Tyr-527), anti-STAT3, anti-phospho-STAT3 (Tyr-705), anti-ERK1/ERK2, anti-phosphospecific ERK1/2 (Thr-202 and Tyr-204), anti-p38 MAPK, anti-phosphospecific p38 MAPK (Thr-180/Tyr-182) and anti-phosphospecific Lck (Tyr-505) (Cell Signaling Technology); anti-JAK2, anti-phosphospecific JAK2 (Tyr-1007 and Tyr-1008), and anti-phosphotyrosine (PY20) (Upstate Biotechnology, Inc.); and anti-Lck and anti-Fyn (Santa Cruz Biotechnology).

LAR-deficient Mice—LAR-deficient mice (kindly provided by Dr. Frank Longo, University of North Carolina, Chapel Hill) were generated by using the gene trap method (33, 34). LAR$^{-/-}$ littermates were derived via heterozygous crosses and were backcrossed at least eight times into the DBA background. Genotyping was done using reverse transcription-PCR as described by Yeo *et al.* (35).

Cell Culture—Aortic VSMCs were isolated from 4-month-old male LAR$^{+/+}$ and LAR$^{-/-}$ mice as previously described by our group (36). Cells were maintained in Dulbecco's modified Eagle's medium (DMEM) containing 10% (v/v) fetal bovine serum (FBS), as described previously (37). Human aortic VSMCs (Cambrex Corp.) were cultured in smooth muscle cell basal medium containing 5% FBS, 100 ng/ml insulin, 200 ng/ml human fibroblast growth factor, 100 ng/ml human epidermal growth factor, 50 μg/ml gentamicin, and 50 ng/ml amphotericin. All experiments were conducted using VSMCs between passages 4 and 11 that were growth-arrested by incubation in DMEM containing 0.1% FBS for 72 h.

Immunoprecipitation and Western Analysis—Cells were lysed either in radioimmune precipitation buffer (20 mM Tris-HCl, pH 7.6, 150 mM NaCl, 0.05 mM sodium fluoride, 1 mM EDTA, 1% Igepal CA-630, 0.05% sodium deoxycholate, and 0.1% sodium dodecyl sulfate) or Triton lysis buffer (20 mM Tris-HCl, pH 7.4, 137 mM NaCl, 2 mM EDTA, 10% glycerol, and 1% Triton X-100) containing protease inhibitors. Immunoprecipitation and Western analysis were performed as described previously (36).

Measurement of LAR Activity—LAR activity was measured using the fluorescence-based RediPlate 96 EnzChek Tyrosine Phosphatase Assay Kit from Molecular Probes. VSMCs were lysed in lysis buffer containing 20 mM Tris-Cl, pH 7.4, 132 mM NaCl, 2 mM EDTA, 10% glycerol, 1% Triton X-100, and a protease inhibitor mixture. Cell lysates containing 500 μg of protein were immunoprecipitated with goat anti-LAR polyclonal antibody overnight at 4 °C, and then incubated with Protein A-Sepharose beads for another 2 h. The immunoprecipitates were washed three times with lysis buffer, and resuspended in 80 μl of assay buffer (20 mM MOPS, pH 7.0, 50 mM NaCl, 1 mM dithiothreitol, and 0.05% Tween 20) containing 50 μM substrate, 6,8-difluoro-4-methylumbelliferyl phosphate. The reaction was performed at 37 °C for 30 min in the dark. 6,8-Difluoro-4-methylumbelliferyl fluorescence was measured at an excitation wavelength of 355 nm and an emission wavelength of 460 nm using a WALLAC 1420 Multilabel Counter. Phosphatase activity was calculated using a 6,8-difluoro-4-methylumbelliferyl phosphate standard curve.

Measurement of Recombinant LAR Activity in the Presence of H$_2$O$_2$—Recombinant LAR activity was assayed by measuring the dephosphorylation of universal phosphatase substrate, *p*-nitrophenyl phosphate. Formation of *p*-nitrophenolate product was monitored in real-time by measuring absorbance at 410 nm in a Beckman BDU-7500 spectrophotometer. All assays were performed at pH 7.0 in a reaction buffer containing 25 mM MOPS, 50 mM NaCl, and 0.05% Tween 20. LAR (6.25 nM) was reacted with 1 mM H$_2$O$_2$ in the absence of reducing agents. The reaction was allowed to proceed for 10 min at 25 °C in the presence of 0.5 mM *p*-nitrophenyl phosphate.

In Vitro Dephosphorylation Assay—Cell lysates obtained from growth-arrested LAR$^{-/-}$ VSMCs, treated with H$_2$O$_2$ for 10 min, were immunoprecipitated with either anti-Fyn or anti-STAT3 antibodies and immobilized on protein A-agarose beads. The beads were washed three times with lysis buffer, and then either left untreated or incubated with purified recombinant LAR (New England Biolabs), in the presence or absence of 0.1 mM sodium orthovanadate, at 30 °C. The reaction was stopped by adding Laemmli sample buffer and boiling for 5 min. Dephosphorylation of tyrosine-phosphorylated immunoprecipitates was observed by Western analysis with anti-PY20 antibody.

Construction of Recombinant Adenoviruses—Adenovirus-encoding LAR (AdLAR) was constructed by subcloning full-length human LAR cDNA (generously provided by Robert A. Mooney, University of Rochester, Rochester, NY) into adenoviral shuttle vector, pShuttle-CMV. After homologous recombination, by electroporation of pShuttle-CMV containing LAR cDNA into BJ5183 *Escherichia coli* (Stratagene) possessing the adenoviral backbone plasmid pADEasy-1, recombinants were selected. Recombinant (E1/E3-deficient) adenoviruses were generated by transfection of human embryonic kidney 293 cells with the recombinant plasmid using Lipofectamine (Invitrogen). Then the virus was serially amplified, purified on a CsCl density gradient by ultracentrifugation, and titered (38). A control adenovirus, consisting of the identical adenovirus backbone with β-galactosidase cDNA insert (Adβ-galactosidase), was provided by Dr. Huang (University of North Carolina, Chapel Hill).

Adenovirus Infection—Adenoviral infection of nearly confluent VSMCs was performed at a multiplicity of infection of 100 in DMEM containing 2% FBS. After 16-h incubation, the cells were made quiescent in DMEM containing 0.1% FBS for 72 h.

Assessment of Apoptosis—For detection of apoptosis, growth-arrested VSMCs were harvested after 16-h treatment with 1 mM H$_2$O$_2$. Histone-associated DNA fragmentation in cell lysates was determined using the Cell Death Detection ELISA^{PLUS} kit (Roche Applied Science) in accordance with the manufacturer's instructions.

Cell death was also assessed by staining H$_2$O$_2$-treated (1 mM H$_2$O$_2$ for 3 h) VSMCs with MitoCapture reagent, a fluorescent lipophilic dye that indicates loss of mitochondrial membrane potential, which is a marker of apoptosis. MitoCapture reagent accumulates and aggregates in the mitochondria of healthy cells fluorescing red (590 nm), whereas in the apoptotic cells it remains in the cytoplasm fluorescing green (530 nm). The pixel intensity of photomicrographs obtained by fluorescent microscopy was quantified using ImageQuaNT software.

Determination of Cell Viability—Cell viability was measured by using a crystal violet staining assay. Cells cultured in 96-well plates at 8000 cells/well were treated with or without H$_2$O$_2$. After 16-h treatment, the media were decanted, and the cells were washed once with phosphate-buffered saline, followed by crystal violet staining (0.5% crystal violet in 1% ethanol and 1.5% formaldehyde) for 30 min. The cells were rinsed with H$_2$O, and the bound dye was solubilized by incubation at 37 °C for 30 min with 100 μl of 1.0% deoxycholate. The absorbance was measured at 550 nm using a WALLAC 1420 Multilabel Counter.

Caspase-3/7 Assay—Caspase-3/7 activities were measured using an Apo-ONE^{TM} Homogeneous Caspase-3/7 Assay kit (Promega). Briefly, cells seeded in 24-well plates at a density of 2.0 × 10^4 cells/well, were grown in DMEM containing 10% FBS, and then starved with serum-free medium for 24 h prior to treatment with 1 mM H$_2$O$_2$ for 2 h. The cells were lysed using a bifunctional cell lysis/activity buffer, which contained a profluorescent caspase-3/7 consensus substrate, rhodamine 110-bis-*N*-CBZ-L-aspartyl-L-glutamyl-L-valyl-L-aspartic acid amide (Z-DEVD-R110). After incubation at room temperature for 1 h, aliquots (150 μl) were transferred to a 96-well clear-bottom plate. Fluorescence was measured at an excitation wavelength of 485 nm and an emission wavelength of 535 nm using a WALLAC 1420 Multilabel Counter.

Retroviral Fyn shRNA Constructs and Infection of Mouse Aortic VSMCs—Two mouse pSM2 retroviral shRNAs for Fyn and one retroviral scrambled shRNA constructs were purchased from Open Biosystems. The sense sequences of Fyn shRNA were 5′-CCGATGTTATGTCAAAGGCCAA-3′ (RMM1766-96740266) and 5′-CCCACACTAACTTCCTG-TATAA-3′ (RMM1766-96740343). The scrambled shRNA encoded a 19-bp sequence (5′-GCGCGCTTTGTAGGAT-TCG-3′) with no significant homology to any mouse gene, and was cloned into pSUPER.retro.puro vector. All retroviruses were prepared in [Phi]Nx-eco cells (Orbigen) by calcium phosphate transfection. Puromycin-resistant clones (selected with 2 μg/ml puromycin for 10 days) were expanded prior to their use in experiments. The effectiveness of Fyn shRNA was confirmed by Western blotting of cell lysates with anti-Fyn antibodies.

Fyn Kinase Assay—After appropriate treatments, cells were washed with cold phosphate-buffered saline, and lysed on ice for 15 min in lysis buffer containing 20 mM HEPES, pH 7.4, 2 mM EGTA, 1 mM dithiothreitol, 50 mM β-glycerophosphate, 1% Triton X-100, 10 units/ml aprotinin, 2 μM leupeptin, 1 mM Na$_3$VO$_4$, and 400 μM phenylmethylsulfonyl fluoride. Cell lysates containing 500 μg of protein were immunoprecipitated with anti-Fyn antibody for 2 h at 4 °C and then incubated with 40 μl of 50% (w/v) protein A-Sepharose beads for an additional 1 h. The beads were washed three times with lysis buffer and resuspended in 30 μl of kinase buffer (20 mM Tris, pH 7.5, 10 mM MnCl$_2$, 10 mM MgCl$_2$) containing 2.5 μg of denatured human non-neuronal enolase, 5 μM ATP, and 5 μCi of [γ-^{32}P]ATP and incubated at 37 °C for 15 min. The reactions were stopped by adding 20 μl of 4× Laemmli sample buffer. The samples were heated at 95 °C for 5 min and analyzed by SDS-gel electrophoresis on 10% acrylamide gels. The dried gel was exposed to x-ray film and developed. Levels of phosphorylated enolase were quantified by densitometry.

Statistical Analysis—All numerical data are expressed as mean ± S.E. Data were analyzed with one-way and two-way analysis of variance (ANOVA) and in case of one-way ANOVA, post-hoc analysis was performed using the Newman-Keuls test. Statistical significance was accepted at $p < 0.05$.

RESULTS

LAR Activity Is Inhibited under Oxidative Stress Condition—Because ROS are known to induce apoptosis by inhibiting PTP activity (39), we investigated whether H$_2$O$_2$ treatment inhibits
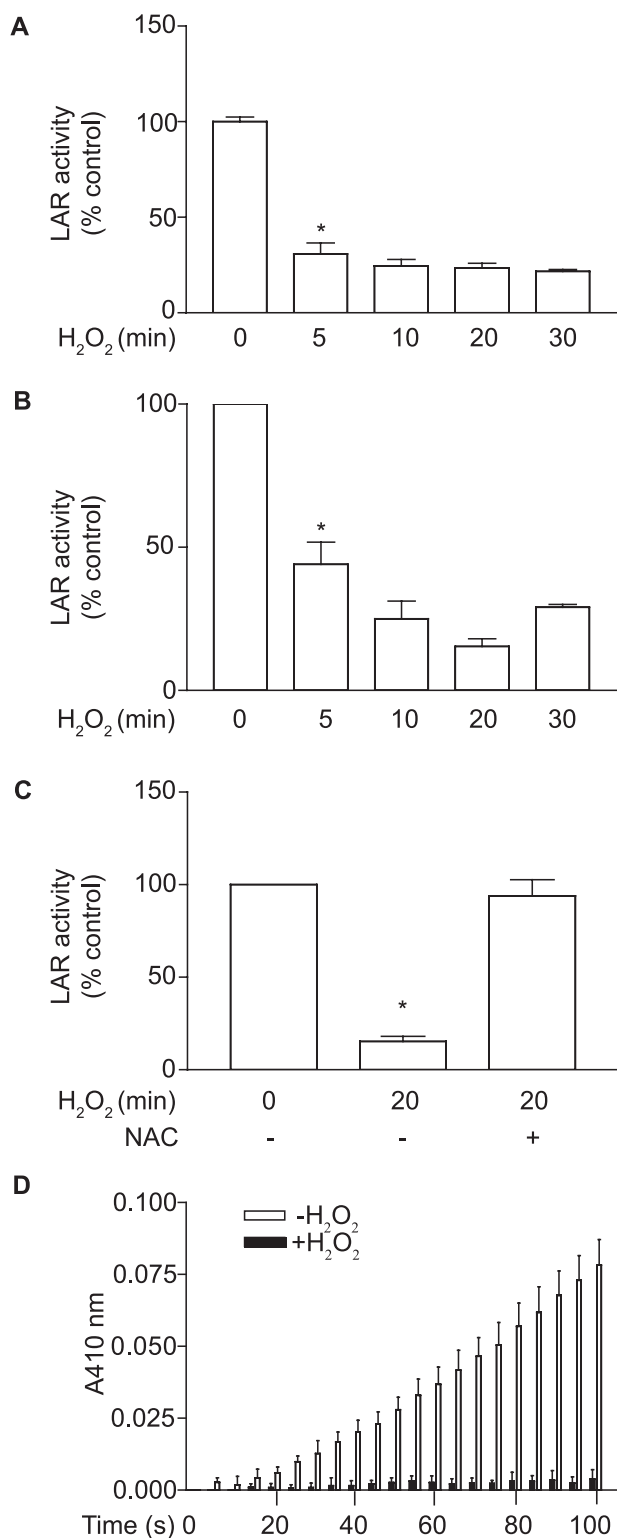
FIGURE 1. **H₂O₂ treatment inactivates LAR in mouse aortic VSMCs.** *A,* growth-arrested VSMCs were treated with 1 mM H₂O₂ for the indicated time, and cell lysates were immunoprecipitated with anti-LAR antibody. Phosphatase activity was measured using 6,8-difluoro-4-methylumbelliferyl phosphate as a substrate. Data presented are mean ± S.E., (*n* = 3) of three separate experiments (*, *p* < 0.001 compared with control). *B,* LAR⁻/⁻ VSMCs, infected with AdLAR, were growth-arrested and then treated with 1 mM H₂O₂ for the indicated times. LAR activity was measured as described above, and data presented are mean ± S.E., (*n* = 3) and representative of three separate experiments (*, *p* < 0.001 compared with control). *C,* LAR activity was assayed in lysates from growth-arrested VSMCs that were pretreated with 10 mM *N*-acetyl cysteine for 60 min and then treated with 1 mM H₂O₂ for 20 min. Data

the activity of LAR in VSMCs. We immunoprecipitated LAR in VSMCs lysates with an antibody raised against the C-terminal cytoplasmic domain of LAR and measured its activity using a Tyrosine Phosphatase Assay Kit (Molecular Probes). A decrease of ~70% in LAR activity (*p* < 0.001) was observed 5 min after treatment with 1 mM H₂O₂ (Fig. 1*A*). LAR activity remained inhibited during the 30-min H₂O₂ treatment. We also measured the effect of H₂O₂ on LAR activity in LAR⁻/⁻ VSMCs expressing AdLAR. LAR activity decreased significantly (*p* < 0.001) 5 min after H₂O₂ treatment, and a maximal inhibition of 80% was observed at 20 min (Fig. 1*B*). Pretreatment with *N*-acetyl cysteine, a thiol-reducing agent, abrogated H₂O₂-induced inhibition of LAR activity (Fig. 1*C*). Further, incubation of recombinant LAR with 1 mM H₂O₂, in the absence of reducing agents, resulted in complete inactivation of this PTP (Fig. 1*D*). These data support the notion that LAR is a redox-sensitive phosphatase, and the residual activity of this PTP in H₂O₂-treated VSMCs might be due to the inherent reducing capacity in VSMCs.

Deficiency of LAR Enhances H₂O₂-induced Apoptosis—ROS are known to induce apoptosis by inhibiting PTP activity (39). Further, H₂O₂-induced VSMC apoptosis is inhibited by Na₃VO₄, an inhibitor of PTP (40). To investigate the role of LAR in oxidative-stress induced apoptosis, we characterized the effect of H₂O₂ on VSMC apoptosis using cells derived from LAR⁺/⁺ (wild-type) and LAR⁻/⁻ (knockout) mice. VSMCs were treated with 1 mM H₂O₂ for 16 h, and apoptosis was assessed by analyzing histone-associated DNA fragmentation from cellular extracts (Fig. 2*A, upper panel*). There was no difference in the basal level apoptosis between wild-type and LAR knockout VSMCs. H₂O₂ significantly increased DNA fragmentation in both wild-type and LAR knockout VSMCs compared with their respective untreated controls. However, apoptosis in response to H₂O₂ was significantly greater in LAR knockout VSMCs compared with the wild-type VSMCs (*p* < 0.001).

To confirm the role of LAR in H₂O₂-induced apoptosis, we measured caspase-3/7 activity (Fig. 2*A, middle panel*), a fairly early marker of apoptosis (41, 42). Caspase-3/7 activity levels were very low in untreated wild-type and LAR knockout VSMCs but increased in both cell types in response to H₂O₂ treatment. The observed increase in caspase-3/7 activity was significantly greater in LAR knockout VSMCs than in wild-type VSMCs following treatment with H₂O₂ for 2 h (*p* < 0.001). Caspase-3/7 activity was much lower in both VSMCs after 16-h treatment with H₂O₂. However, LAR knockout VSMCs had significantly higher (*p* < 0.001) caspase-3/7 activity than wild-type cells 16 h after H₂O₂ treatment (data not shown). These results indicate that deficiency of LAR results in hyperactivation of cellular signaling pathways that cause apoptosis under oxidative stress conditions.

We further confirmed that absence of LAR enhances H₂O₂-induced VSMC apoptosis by measuring changes in mitochondrial membrane potential using MitoCapture reagent (Fig.

presented are mean ± S.E. (*n* = 3) of three separate experiments (*, *p* < 0.001 compared with control). *D,* the catalytic activity of recombinant LAR, in the absence of reducing agents, was assayed by monitoring the increase in absorbance resulting from the hydrolysis of substrate, *p*-nitrophenyl phosphate. A significant change in activity was observed for time and treatment (two-way ANOVA, *p* < 0.0001).
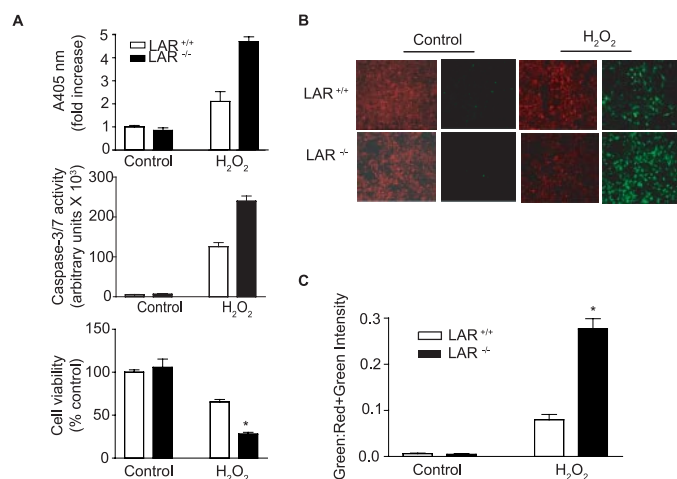
FIGURE 2. **LAR deficiency increases H$_2$O$_2$-induced apoptosis and caspase-3/7 activity, and decreases cell viability in VSMCs.** *A,* growth-arrested VSMCs were treated with 1 mM H$_2$O$_2$ for 16 and 2 h, and lysates were used to measure histone-associated DNA fragmentation (*upper panel*) and caspase-3/7 activity (*middle panel*), respectively. Viability of VSMCs treated with 1 mM H$_2$O$_2$ for 16 h was assayed by staining with crystal violet (*lower panel*). The absorbance was measured at 550 nm, and cell survival data are expressed as percent of untreated cells (mean ± S.E., *n* = 3; *, *p* < 0.01 compared with LAR$^{+/+}$ VSMCs treated with H$_2$O$_2$). *B,* H$_2$O$_2$-induced apoptosis as measured by mitochondrial membrane injury. VSMCs were either untreated or treated with 1 mM H$_2$O$_2$ for 3 h, and then stained with MitoCapture reagent and visualized using a fluorescence microscope. Predominant red staining is indicative of healthy cells, whereas predominant green staining indicates apoptotic cells. *C,* pixel intensity of MitoCapture-treated LAR$^{+/+}$ and LAR$^{-/-}$ cells was determined, and the data are presented as the ratio of green to red plus green pixel intensity (mean ± S.E., *n* = 3; *, *p* < 0.001 compared with wild-type cells treated with H$_2$O$_2$).

2*B*). VSMCs were treated with or without 1 mM H$_2$O$_2$ for 3 h prior to MitoCapture staining. In untreated wild-type and LAR knockout VSMCs, the fluorescence of MitoCapture was red indicating mitochondrial accumulation and healthy cells. Following H$_2$O$_2$ treatment, increase in green fluorescence was evident in both wild-type and LAR knockout cells, indicating apoptosis. Consistent with other markers of apoptosis, the ratio of green-to-red plus green fluorescence was significantly higher in LAR knockout VSMCs than in wild-type VSMCs (*p* < 0.001) (Fig. 2*C*).

Finally, we tested whether the increase in apoptosis after H$_2$O$_2$ treatment was associated with the decrease in VSMC viability using crystal violet staining (Fig. 2*A*, *lower panel*). Viability decreased significantly in wild-type cells after H$_2$O$_2$ treatment (*p* < 0.01). However, cell viability was significantly lower in LAR knockout VSMCs than in wild-type VSMCs, following H$_2$O$_2$ treatment (*p* < 0.01). Together, these data indicate that LAR regulates the apoptotic pathways in VSMCs and plays an important role in protecting these cells from oxidative stress-induced death.

Deficiency of LAR Enhances H$_2$O$_2$-induced Tyrosine Phosphorylation of Fyn but Not Lck and c-Src—Berk and colleagues (43, 44) previously demonstrated the activation of Src family kinases in ROS-initiated signaling events. It was reported that Fyn, a Src family kinase, is required for H$_2$O$_2$-mediated activation of intracellular signaling events (45). Further, it was recently demonstrated that LAR binds both Fyn and Lck, another Src family kinase, and that LAR dephosphorylates Fyn both *in vitro* and in thymocytes (46). To determine whether

LAR deficiency has differential effects on activation of Fyn and other Src family kinases, Lck and c-Src, we analyzed tyrosine phosphorylation of these kinases in cellular extracts of wild-type and LAR knockout VSMCs treated with 1 mM H$_2$O$_2$. Tyrosine phosphorylation of Fyn and c-Src was assessed by immunoprecipitation of cell lysates with their respective antibodies and then probing the immunoprecipitates with anti-phosphotyrosine (PY20) antibody, whereas Lck tyrosine phosphorylation was assessed by immunoblotting the cell lysates with anti-phosphospecific Lck antibody. A significant increase in Fyn tyrosine phosphorylation was observed with time and cell type (*p* < 0.0001, two-way ANOVA) in response to H$_2$O$_2$ treatment (Fig. 3, *A* and *B*). Sustained increase in Lck and c-Src phosphorylation was observed with time in both cell types when treated with H$_2$O$_2$ (*p* < 0.0001 for each kinase, two-way ANOVA) (Fig. 3, *C–F*). However, there was no significant difference in tyrosine phosphorylation of Lck and c-Src between wild-type and LAR knockout VSMCs (Fig. 3, *D* and *E*). It is unlikely that other PTPs are compensating/regulating the phosphorylation of these kinases in the absence of LAR, because LAR knockout mice did not exhibit any changes in the expression of other LAR family PTPs (47), and we did not observe any difference in the activity of a related PTP, PTP1B, between LAR$^{+/+}$ and LAR$^{-/-}$ VSMCs (data not shown). Although we do not know the exact mechanism, our results indicate that LAR specifically regulates H$_2$O$_2$-induced Fyn, but not Lck and c-Src in VSMCs, through tyrosine phosphorylation.

H$_2$O$_2$ Treatment Increases Autophosphorylation of Tyr-419 and Activity of Fyn Kinase in LAR-deficient VSMCs—Fyn contains two tyrosine phosphorylation sites, Tyr-419, an autophosphorylation site in the tyrosine kinase domain, and Tyr-530, a regulatory phosphorylation site within the C terminus (46). Autophosphorylation of Tyr-419 increases kinase activity, whereas phosphorylation of Tyr-530 inhibits the kinase via an intramolecular interaction with the SH2 domain (48, 49). To determine whether absence of LAR results in increased autophosphorylation of Fyn in cells treated with H$_2$O$_2$, we immunoprecipitated Fyn and probed Tyr-419 phosphorylation using phosphospecific anti-Src (pY416) antibody, which cross-reacts with autophosphorylated Fyn kinase. Fyn autophosphorylation increased significantly, but transiently 5 min after H$_2$O$_2$ treatment (*p* < 0.05 *versus* respective control) in wild-type VSMCs (Fig. 4*A*). However, the absence of LAR caused significant and sustained increase in autophosphorylation of Fyn in VSMCs treated with H$_2$O$_2$ (*p* < 0.001 *versus* untreated LAR knockout VSMCs and wild-type VSMCs following H$_2$O$_2$ treatment).

Next, we examined the effect of H$_2$O$_2$ on phosphorylation of Fyn Tyr-530 by immunoprecipitating the VSMC lysates with anti-Fyn antibody, followed by Western analysis with phosphospecific anti-Src (pY527) antibody, which cross-reacts with phosphorylated Fyn Tyr-530. Consistent with the report of Sanguinetti *et al.* (49), H$_2$O$_2$ treatment of wild-type VSMCs increased phosphorylation of Fyn on its inhibitory Tyr residue in the C terminus (*p* < 0.05 at 5 min *versus* untreated cells) (Fig. 4*B*). Phosphorylation of Fyn Tyr-530 was significantly higher in LAR$^{-/-}$ VSMCs than in wild-type VSMCs 10, 20, and 30 min after H$_2$O$_2$ treatment (*p* < 0.001 for each time point).
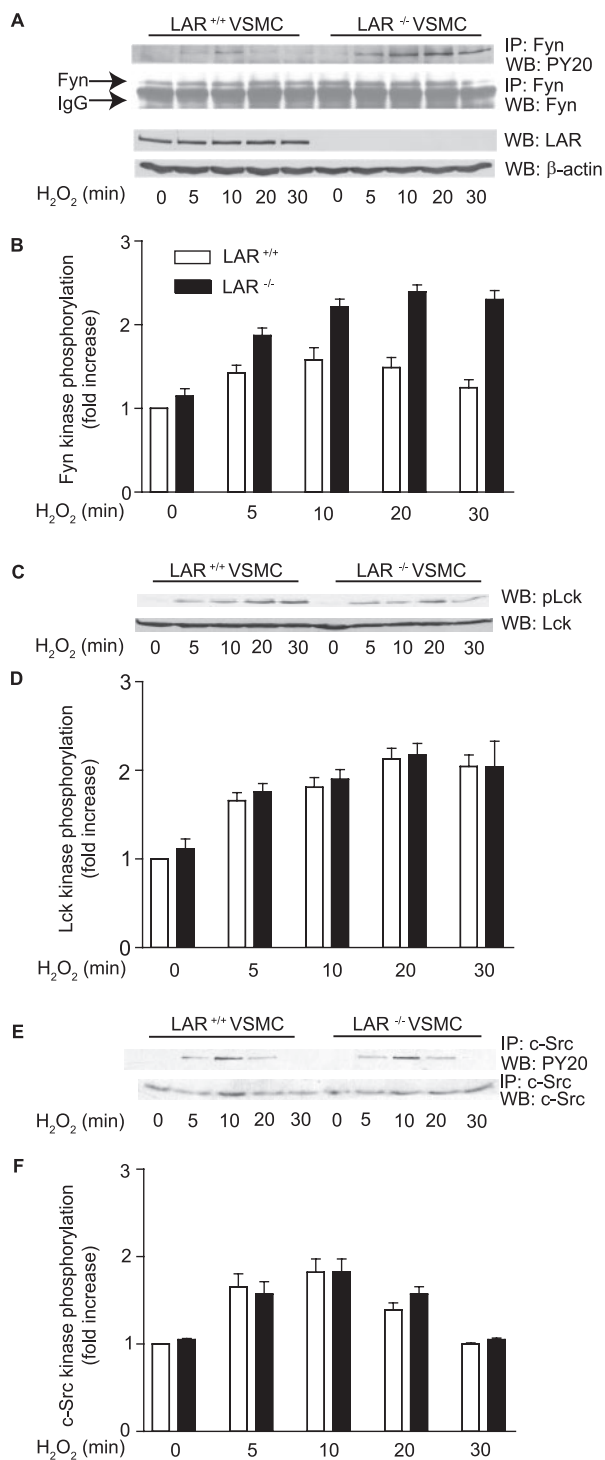
FIGURE 3. **LAR deficiency increases tyrosine phosphorylation of Fyn.** *A*, VSMCs were either left untreated or treated with 1 mM H₂O₂, and the cell lysates containing equal amounts of protein were immunoprecipitated with anti-Fyn antibody followed by Western analysis with either anti-phosphotyrosine (PY20) antibody or anti-Fyn antibody. Cell lysates were also analyzed by Western blotting with anti-LAR monoclonal antibody, and the membrane was reprobed with anti-β-actin antibody. *B*, densitometric analysis of normalized Fyn phosphorylation (mean ± S.E., *n* = 3; *p* < 0.0001 for cell type and time in two-way ANOVA). *C*, VSMCs were stimulated with 1 mM H₂O₂, and cell lysates were analyzed by Western blotting with either anti-phospho Lck or anti-Lck antibody. *D*, densitometric analysis of normalized Lck phosphorylation (mean ± S.E., *n* = 3; *p* < 0.0001 for time in two-way ANOVA). *E*, H₂O₂-treated VSMC lysates were immunoprecipitated with anti-c-Src antibody followed by Western analysis with either anti-PY20 antibody or anti-c-Src antibody. *F*, densitometric analysis of normalized c-Src phosphorylation (mean ± S.E., *n* = 3; *p* < 0.0001 for time in two-way ANOVA).
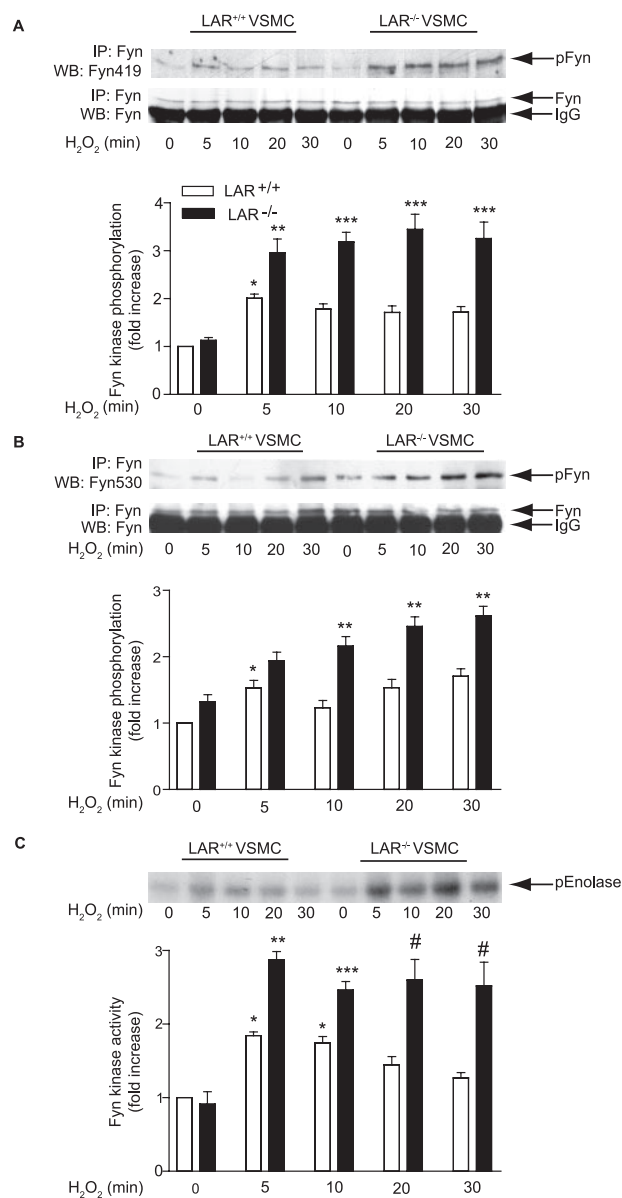

FIGURE 4. **H₂O₂-induced Fyn autophosphorylation and kinase activity are enhanced in the absence of LAR.** *A*, growth-arrested LAR⁺/⁺ and LAR⁻/⁻ VSMCs were either left untreated or treated with 1 mM H₂O₂ for the indicated times, and the cell lysates were immunoprecipitated with anti-Fyn antibody followed by Western analysis with anti-phosphospecific Fyn (pY419) antibody (*top panel*). The membrane was reprobed with anti-Fyn antibody (*middle panel*). Densitometric analysis (*lower panel*) of Fyn autophosphorylation (mean ± S.E., *n* = 3; *, *p* < 0.05 *versus* untreated LAR⁺/⁺ VSMCs, **, *p* < 0.01 *versus* respective control, ***, *p* < 0.001 *versus* respective control). *B*, lysates from VSMCs, treated as described above, were immunoprecipitated with anti-Fyn antibody followed by Western analysis with anti-phosphospecific Fyn (pY530) antibody (*top panel*). The membrane was reprobed with anti-Fyn antibody (*middle panel*). Densitometric analysis (*lower panel*) of Fyn (pY530) phosphorylation (mean ± S.E., *n* = 3; *, *p* < 0.05 *versus* LAR⁺/⁺ VSMCs, **, *p* < 0.001 *versus* respective control). *C*, growth-arrested VSMCs were treated with 1 mM H₂O₂ for the indicated times. Cell lysates containing equal amount of protein were immunoprecipitated with anti-Fyn antibody, and Fyn kinase activity was measured by an immunocomplex kinase assay using denatured enolase as the substrate (*top panel*). Densitometric analysis (*lower panel*) of Fyn activity (mean ± S.E., *n* = 3; *, *p* < 0.05 *versus* untreated LAR⁺/⁺ VSMCs; ** *p* < 0.05 *versus* respective control; ***, *p* < 0.05 *versus* respective control; #, *p* < 0.001 *versus* respective control).

Because LAR deficiency resulted in increase in both the autophosphorylation as well as phosphorylation of inhibitory Fyn Tyr-530 residue, we measured Fyn activity in untreated and
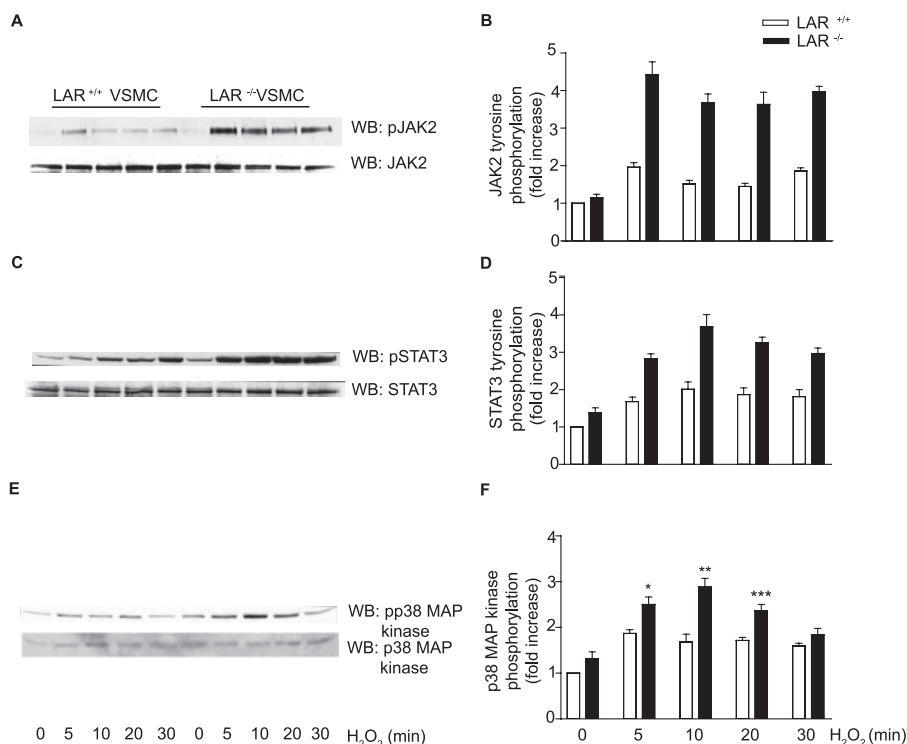
FIGURE 5. JAK2, STAT3, and p38 MAPK phosphorylation are enhanced in the absence of LAR. Growth-arrested $LAR^{+/+}$ and $LAR^{-/-}$ VSMCs were either left untreated or treated with 1 mM H_2O_2, and phosphorylation was determined by immunoblotting with either anti-phospho JAK2 (*A*), anti-phospho STAT3 (*C*), or anti-phospho p38 MAPK (*E*) antibodies. Densitometric analysis of normalized phospho JAK2 (*B*), phospho STAT3 (*D*), and phospho p38 MAPK (*F*) (mean ± S.E., $n = 3$; *, $p < 0.01$, **, $p < 0.001$, and ***, $p < 0.05$ *versus* respective controls).
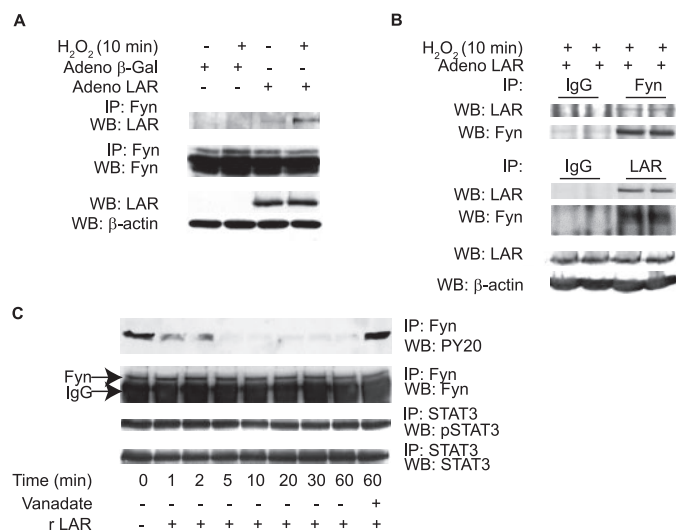

FIGURE 6. LAR associates with and dephosphorylates activated Fyn. *A*, lysates from growth-arrested $LAR^{-/-}$ VSMCs, either untreated or treated with 1 mM H_2O_2 in the presence of Adβ-galactosidase or AdLAR, were immunoprecipitated with anti-Fyn antibody and Western analysis was performed with anti-LAR antibody. The membrane was reprobed with anti-Fyn antibody. LAR overexpression was confirmed by Western analysis of cell lysates with either anti-LAR or anti-β-actin antibody (loading control). *B*, growth-arrested $LAR^{-/-}$ VSMCs infected with AdLAR were treated with H_2O_2, and cell lysates were immunoprecipitated with either anti-Fyn or anti-LAR antibodies or isotype-matched control antibodies. Western analysis was done with either anti-LAR (the membrane was reprobed with anti-Fyn) or anti-Fyn (membrane reprobed with anti-LAR) antibodies. LAR overexpression was confirmed as described above. *C*, Fyn or STAT3 were immunoprecipitated from lysates of VSMCs treated with H_2O_2, immobilized on protein A-agarose beads, and incubated with recombinant LAR in the phosphatase reaction buffer. Phosphorylation was examined with either anti-PY20 or anti-phospho STAT3 (Tyr-705) antibodies. Equal loading of Fyn and STAT3 in cell lysates was confirmed by immunoprecipitation/Western analysis of aliquots with respective antibodies.

H_2O_2-treated VSMCs using an immunocomplex kinase assay with enolase as the substrate. Fyn kinase activity, after H_2O_2 treatment, increased significantly in wild-type VSMCs for 10 min ($p < 0.05$ *versus* untreated control) (Fig. 4*C*). However, the activity of Fyn kinase decreased thereafter and returned to near basal levels 30 min after H_2O_2 treatment. Fyn kinase activity in LAR knockout VSMCs was significantly higher under basal conditions ($p < 0.05$ *versus* untreated wild type) and increased further with H_2O_2 treatment ($p < 0.05$ 30 min after treatment *versus* untreated LAR knockout VSMCs). Deficiency of LAR resulted in significant and sustained activation of Fyn kinase after H_2O_2 treatment ($p < 0.001$ *versus* wild-type VSMCs 30 min after H_2O_2 treatment). Together, these data indicate that increase in autophosphorylation overrides the increase in phosphorylation of inhibitory Tyr-530 residue in modulating Fyn activity in the absence of LAR.

Enhanced Activation of JAK2-STAT3 Pathway and p38 MAPK in H_2O_2-treated LAR-deficient VSMCs—Fyn is required for H_2O_2-mediated activation of Janus kinase 2 (JAK2) (43), which is essential for H_2O_2-induced apoptosis (50). Therefore, we investigated whether sustained activation of Fyn by H_2O_2 in LAR knockout cells would result in higher activation of JAK2 as well. Western analysis with phosphospecific antibodies demonstrated a significant increase in JAK2 phosphorylation with time and cell type in VSMCs treated with H_2O_2 ($p < 0.0001$, two-way ANOVA) (Fig. 5, *A* and *B*). To determine whether enhanced activation of JAK2 in LAR knockout VSMCs treated with H_2O_2 leads to tyrosine phosphorylation of STAT3, a JAK2 substrate, we measured STAT3 tyrosine phosphorylation in wild-type and LAR knockout VSMCs treated with H_2O_2 (Fig. 5*C*). H_2O_2 treatment caused a significant increase in STAT3 tyrosine phosphorylation with time and cell type ($p < 0.0001$, two-way ANOVA) in VSMCs (Fig. 5*D*).

Fyn tyrosine kinase is upstream of p38 MAPK in the signal transduction pathways of several cells, including vascular cells (51, 52). Because the activation of p38 MAPK has been implicated in apoptosis of VSMCs (53, 54), we examined the activation of this kinase in wild-type and LAR knockout VSMCs treated with H_2O_2 (Fig. 5*E*). Phosphorylation of p38 MAPK was significantly higher in LAR knockout VSMCs than in wild-type cells 5 ($p < 0.01$), 10 ($p < 0.001$), and 20 min ($p < 0.05$) after H_2O_2 treatment (Fig. 5*F*).

LAR Binds to and Dephosphorylates Activated Fyn—Because Fyn kinase tyrosine phosphorylation was increased in LAR knockout VSMCs and LAR was shown to bind Fyn in other cell
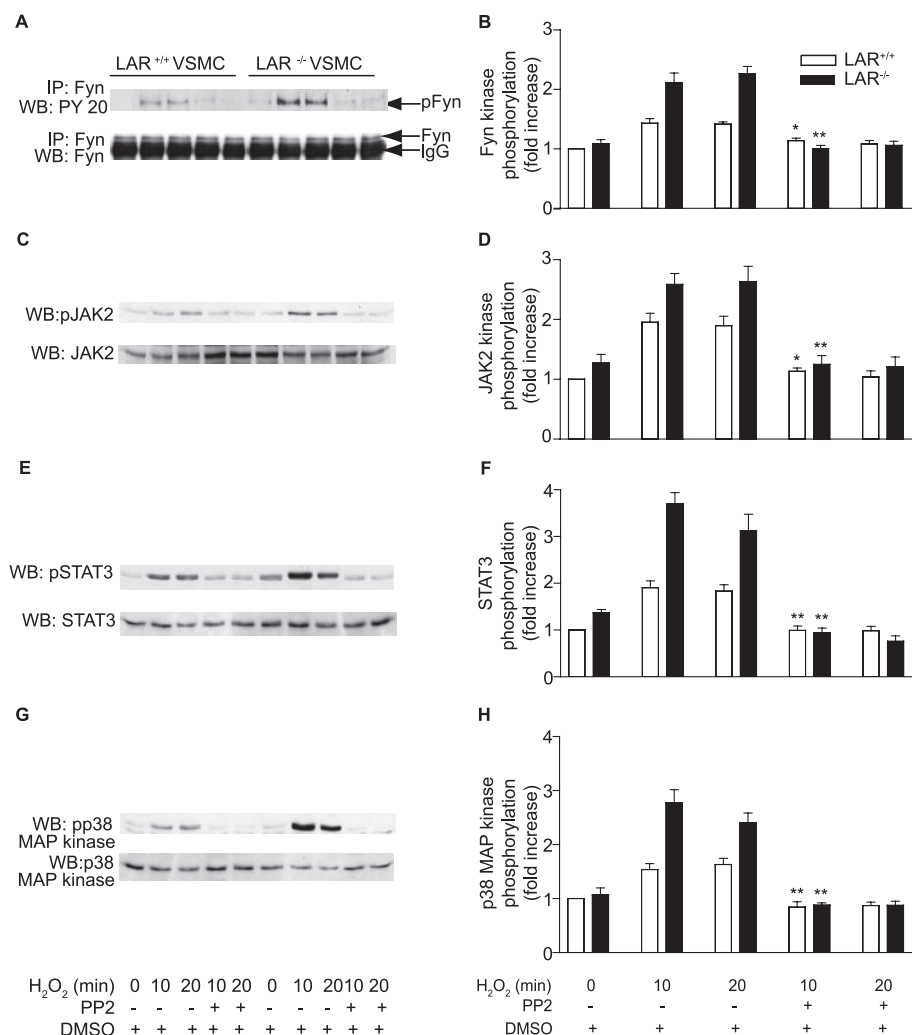
FIGURE 7. **H$_2$O$_2$-induced Fyn and JAK-STAT pathway and p38 MAPK activation is abrogated by a Fyn inhibitor.** Growth-arrested VSMCs were pretreated with DMSO or PP2 (1 μM) for 2 h before treatment with 1 mM H$_2$O$_2$ for the indicated times. Lysates were immunoprecipitated with anti-Fyn antibody and subjected to Western analysis with anti-PY20 antibody (*A*). Lysates were subjected to Western analysis with either anti-phospho Jak2 (*C*), anti-phospho STAT3 (*E*), or anti-phospho p38 MAPK (*G*) antibodies. Densitometric analysis of normalized phospho Fyn (*B*), phospho JAK2 (*D*), and phospho STAT3 (*F*) and phospho p38 MAPK (*H*) (mean ± S.E., *n* = 3; *, *p* < 0.05, and **, *p* < 0.001 *versus* respective cells treated with H$_2$O$_2$ for 10 min).

min, and activated Fyn in the lysates was immunoprecipitated with anti-Fyn antibody and incubated with purified recombinant LAR (New England Biolabs) or vehicle. As shown in Fig. 6C (*upper panel*), Western analysis of immunoprecipitates with anti-PY20 antibody indicated that recombinant LAR dephosphorylated Fyn in a time-dependent manner. Fyn tyrosine dephosphorylation by LAR was inhibited in the presence of sodium vanadate, a potent inhibitor of PTP. In contrast, LAR did not dephosphorylate activated STAT3 immunoprecipitated from LAR knockout VSMCs treated with H$_2$O$_2$ (Fig. 6C, *lower two panels*). Taken together, these results suggest that activated Fyn is a possible substrate of LAR *in vivo* under oxidative stress conditions. Furthermore, LAR mainly regulates the activity of Fyn kinase by modulating autophosphorylation of Tyr-419 in the kinase domain.

Src Family-selective Tyrosine Kinase Antagonist PP2 Inhibits H$_2$O$_2$-induced JAK2, STAT3, and p38 MAPK Phosphorylation—Because Fyn has been suggested to be upstream of JAK2 and p38 MAPK (43, 51, 52), we investigated whether Fyn activation is required for H$_2$O$_2$-induced stimulation of JAK2, STAT3, and p38 MAPKs in VSMCs (Fig. 7). Pretreatment of VSMCs with 1 μM PP2 abrogated H$_2$O$_2$-induced tyrosine phosphorylation of Fyn in wild-type VSMCs (*p* < 0.05 *versus* H$_2$O$_2$ treatment for 10 min, Fig. 7, *A* and *B*). H$_2$O$_2$-induced Fyn tyrosine phosphorylation in LAR$^{-/-}$ VSMCs was also significantly (*p* < 0.001 *versus* H$_2$O$_2$ treatment for 10 min) inhibited by PP2 pretreatment. Similarly, complete inhibition of H$_2$O$_2$-induced tyrosine phosphorylation of JAK2 was observed with PP2 pretreatment in both wild-type (*p* < 0.05 *versus* H$_2$O$_2$ treatment for 10 min) and LAR knockout VSMCs (*p* < 0.001 *versus* H$_2$O$_2$ treatment for 10 min, Fig. 7, *C* and *D*). Consistent with the inhibition of JAK2 activation, PP2 pretreatment significantly decreased H$_2$O$_2$-induced STAT3 tyrosine phosphorylation in both wild-type and LAR$^{-/-}$ VSMCs (*p* < 0.001 *versus* H$_2$O$_2$ treatment for 10 min for both the cell types) (Fig. 7, *E* and *F*). PP2 pretreatment also significantly inhibited H$_2$O$_2$-induced phosphorylation of p38 MAPK in both wild-type and LAR$^{-/-}$ VSMCs (*p* < 0.001 *versus* H$_2$O$_2$ treatment for 10 min for both the cell types) (Fig. 7, *G* and *H*). These data indicate that Fyn activation regulates H$_2$O$_2$-induced signal-

types (46), we investigated whether the regulatory function of LAR on Fyn is mediated by a direct physical interaction between the two proteins in VSMCs treated with H$_2$O$_2$. LAR knockout VSMCs, infected with either human AdLAR or Adβ-galactosidase, were treated with or without H$_2$O$_2$ for 10 min. Immunoprecipitation of these cell lysates with anti-Fyn antibody followed by Western analysis with anti-LAR C-terminal antibody revealed enhanced association of LAR with activated Fyn kinase in VSMCs following treatment with H$_2$O$_2$ (Fig. 6A). The association of LAR with activated Fyn was corroborated using lysates from LAR knockout VSMCs infected with human AdLAR and treated with H$_2$O$_2$. Immunoprecipitation of cell lysates with anti-Fyn antibody followed by Western analysis with anti-LAR C-terminal antibody and reciprocal immunoprecipitation with anti-LAR C-terminal antibody and Western analysis with Fyn antibody confirmed enhanced association of LAR with activated Fyn (Fig. 6B).

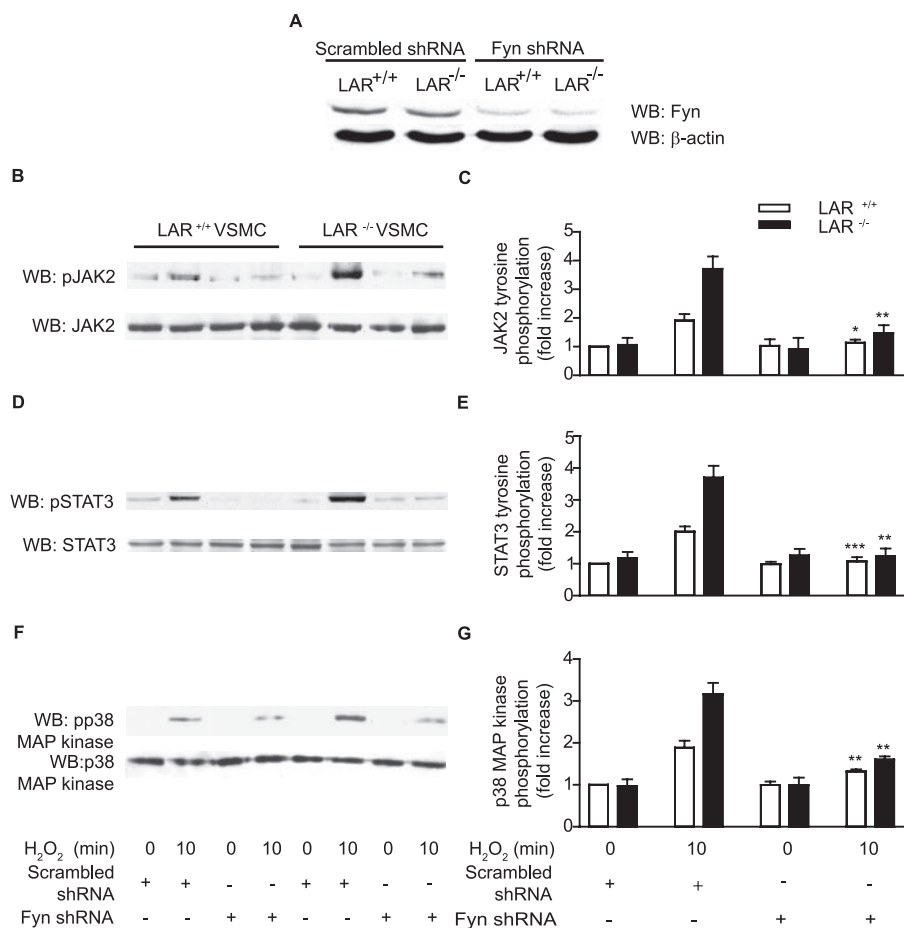Next we examined whether LAR dephosphorylates Fyn *in vitro*. LAR knockout VSMCs were treated with H$_2$O$_2$ for 10

FIGURE 8. **H₂O₂-stimulated tyrosine phosphorylation of JAK2 and STAT3 and p38 MAPK are inhibited in Fyn shRNA-expressing LAR⁺/⁺ and LAR⁻/⁻ VSMC clones.** Scrambled shRNA- or Fyn shRNA-expressing LAR⁺/⁺ and LAR⁻/⁻ VSMCs lysates were analyzed by Western analysis with anti-Fyn antibody, and the membrane was reprobed with anti-β-actin antibody (*A*). Scrambled shRNA- or Fyn shRNA-expressing LAR⁺/⁺ and LAR⁻/⁻ VSMCs clones were growth-arrested and then treated with 1 mM H₂O₂ for the time indicated, and lysates were analyzed by Western blotting with either anti-phospho JAK2 (*B*), anti-phospho STAT3 (*D*), or anti-phospho p38 MAPK (*F*) antibodies. Densitometric analysis of normalized phospho JAK2 (*C*), phospho STAT3 (*E*), and phospho p38 MAPK (*G*) (mean ± S.E., n = 3; *, $p < 0.01$, **, $p < 0.001$ and ***, $p < 0.05$ *versus* respective cells treated H₂O₂ for 10 min).

ing events, and Fyn is an upstream kinase in the JAK-STAT pathway and p38 MAPK activation.

Silencing of Fyn Expression by shRNA Abrogates H₂O₂-induced JAK2, STAT3, and p38 MAPK Phosphorylation in VSMCs—To confirm the requirement for Fyn in H₂O₂-induced JAK2, STAT3, and p38 MAPK activation, we used retroviral expression of Fyn shRNAmir to silence the expression of the endogenous Fyn. Infection of wild-type and LAR⁻/⁻ VSMCs with retroviral Fyn shRNA construct decreased Fyn expression by ~70% compared with respective scrambled shRNA-expressing VSMCs (Fig. 8*A*). Expression of Fyn shRNA abrogated H₂O₂-induced increase in JAK2 phosphorylation in wild-type ($p < 0.01$ *versus* respective scrambled shRNA-expressing cells treated with H₂O₂ for 10 min) and LAR⁻/⁻ VSMCs ($p < 0.001$ *versus* respective scrambled shRNA-expressing cells treated with H₂O₂ for 10 min) (Fig. 8, *B* and *C*). Consistent with JAK2 inhibition, Fyn shRNA expression inhibited H₂O₂-induced increase in STAT3 phosphorylation in wild-type ($p < 0.05$ *versus* respective scrambled shRNA-expressing cells treated with H₂O₂ for 10 min) and LAR⁻/⁻ VSMCs ($p < 0.001$ *versus*

respective scrambled shRNA-expressing cells treated with H₂O₂ for 10 min) (Fig. 8, *D* and *E*). Expression of Fyn shRNA also significantly decreased H₂O₂-induced increase in p38 MAPK phosphorylation in wild-type ($p < 0.001$ *versus* respective scrambled shRNA-expressing cells treated with H₂O₂ for 10 min) and LAR⁻/⁻ VSMCs ($p < 0.001$ *versus* respective scrambled shRNA-expressing cells treated with H₂O₂ for 10 min) (Fig. 8, *F* and *G*). However, expression of Fyn shRNA had no effect on the steady-state levels of JAK2, STAT3, and p38 MAPK expression. Together, these data indicate that LAR regulates H₂O₂-induced cell signaling in VSMCs by modulating Fyn activation.

JAK2 Activates STAT3, but Not p38 MAPK, in VSMCs Treated with H₂O₂—To determine whether JAK2 is upstream of STAT3 as well as p38 MAPK activation, we investigated the effect of AG490, a JAK2-specific inhibitor, on the activation of STAT3 and p38 MAPK in wild-type and LAR knockout VSMCs treated with H₂O₂. Pretreatment with 25 µM AG490 for 16 h prior to H₂O₂ treatment had no effect on phosphorylation of Fyn, the JAK2 upstream kinase, in wild-type and LAR⁻/⁻ cells (Fig. 9, *A* and *B*). Pretreatment with AG490 significantly inhibited H₂O₂-induced tyrosine phosphorylation of JAK2 in both wild-type ($p < 0.05$ *versus* respective cells treated with H₂O₂ for 10 min) and LAR knockout ($p < 0.001$ *versus* respective cells treated with H₂O₂ for 10 min) VSMCs (Fig. 9, *C* and *D*). Consistent with the inhibition of JAK2 stimulation, STAT3 tyrosine phosphorylation was significantly inhibited in both wild-type ($p < 0.05$ *versus* respective cells treated with H₂O₂ for 10 min) and LAR knockout ($p < 0.001$ *versus* respective H₂O₂-treated cells) VSMCs (Fig. 9, *E* and *F*). In contrast, p38 MAPK phosphorylation induced by H₂O₂ was unaffected by AG490 in both the cell types (Fig. 9, *G* and *H*). These results indicate that LAR regulates two alternative oxidative stress-induced pathways in VSMCs: a Fyn/JAK2/STAT3 pathway and a Fyn/p38 MAPK pathway.

Fyn and JAK2 Are Required for H₂O₂-induced Apoptosis of VSMCs—To elucidate the role of Fyn activation in H₂O₂-induced VSMC apoptosis, we pretreated wild-type and LAR knockout VSMCs with Fyn inhibitor PP2 (1 µM) for 2 h, prior to treatment with or without H₂O₂ for 16 h (Fig. 10*A*). PP2 pretreatment significantly decreased H₂O₂-induced apoptosis, as measured by histone-associated DNA fragmentation, in both
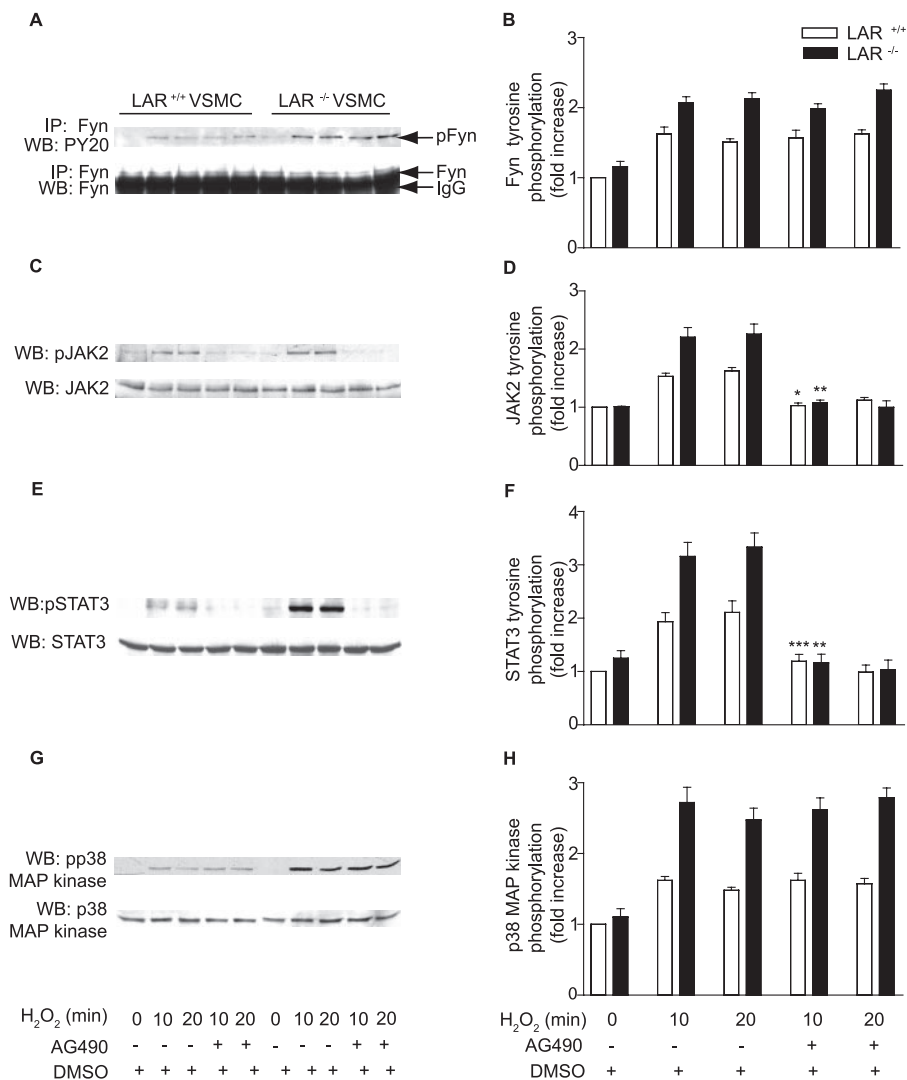
FIGURE 9. H$_2$O$_2$-stimulated tyrosine phosphorylation of JAK2 and STAT3 but not Fyn and p38 MAPK are inhibited by AG490 in both LAR$^{+/+}$ and LAR$^{-/-}$ VSMCs. Growth-arrested VSMCs were pretreated with 25 μM AG490 for 16 h and then treated with H$_2$O$_2$ for 10 min. Cell lysates were immunoprecipitated with anti-Fyn antibody followed by Western analysis with anti-phosphotyrosine (PY20) or anti-Fyn antibody (*A*). Cell lysates were also analyzed by Western blotting with either anti-phospho JAK2 (*C*), anti-phospho STAT3 (*E*), or anti-phospho p38 MAPK (*G*) antibodies. Densitometric analysis of normalized phospho Fyn (*B*), JAK2 (*D*), phospho STAT3 (*F*) and phospho p38 MAPK (*H*) (mean ± S.E., n = 3, *, $p < 0.05$, **, $p < 0.001$ and ***, $p < 0.05$ *versus* respective cells treated with H$_2$O$_2$).

Together, these results indicate that LAR regulates H$_2$O$_2$-induced apoptosis by modulating Fyn kinase activity.

Similar to the effect of PP2 on H$_2$O$_2$-induced apoptosis, pretreatment of VSMCs with 25 μM AG490 for 16 h significantly decreased H$_2$O$_2$-induced histone-associated DNA fragmentation in wild-type and LAR knockout VSMCs ($p < 0.001$ *versus* respective cells treated with H$_2$O$_2$) (Fig. 10*C*). Overall, these results suggest that LAR regulates VSMC apoptosis under oxidative stress conditions by inhibiting hyperactivation of Fyn/JAK2/STAT3 and Fyn/p38 MAPK pathways.

LAR Overexpression Attenuates H$_2$O$_2$-induced Fyn Activation in LAR-deficient VSMCs—To confirm the regulatory role of LAR in Fyn activation induced by H$_2$O$_2$, LAR knockout VSMCs were infected with either Adβ-galactosidase or AdLAR and then treated with H$_2$O$_2$. As shown in Fig. 11, overexpression of LAR in LAR knockout VSMCs led to enhanced association of LAR with activated Fyn (*top panel*) and decreased tyrosine phosphorylation of Fyn kinase (*second panel*). Increased association of LAR with Fyn and decreased phosphorylation of Fyn were also observed in human aortic SMC overexpressing LAR and treated with H$_2$O$_2$ (data not shown). Together, these results support the notion that LAR regulates Fyn activity in VSMCs under oxidative stress conditions.

DISCUSSION

ROS regulate various redox-sensitive cellular functions, including response to stress or growth signals (55). H$_2$O$_2$ is produced during activation of cognate receptors by various growth factors, cytokines, and hormones. The transient increase in intracellular H$_2$O$_2$ produced under these conditions is equivalent to exogenously added H$_2$O$_2$ concentrations of 0.1–1.0 mM (22, 56). When H$_2$O$_2$ is applied to cell cultures, a rapid equilibrium is established, from the metabolic actions of cellular peroxidases and catalases, in which the intracellular concentration of H$_2$O$_2$ is ~7- to 10-fold less than the extracellular concentration (56). PTPs are the important redox sensors inside the cell, because localized reversible oxidation and consequent inactivation of these proteins

wild-type and LAR knockout VSMCs ($p < 0.001$ *versus* respective cells treated with H$_2$O$_2$).

Consistent with the effect of PP2 on H$_2$O$_2$-induced apoptosis in VSMCs, histone-associated DNA fragmentation upon H$_2$O$_2$ treatment was partially, but significantly decreased in wild-type VSMCs clones expressing Fyn shRNA compared with untreated wild-type cells or scrambled shRNA-expressing wild-type VSMCs clones ($p < 0.01$) (Fig. 10*B*). Similarly, a significant decrease in histone-associated DNA fragmentation upon H$_2$O$_2$ treatment was observed in LAR knockout VSMCs clones expressing Fyn shRNA compared with H$_2$O$_2$-treated LAR knockout VSMCs or scrambled shRNA expressing LAR knockout VSMCs clones ($p < 0.001$). Importantly, suppression of Fyn expression in LAR knockout VSMCs decreased H$_2$O$_2$-induced histone-associated DNA fragmentation to the same level observed in wild-type VSMCs clones expressing Fyn shRNA.
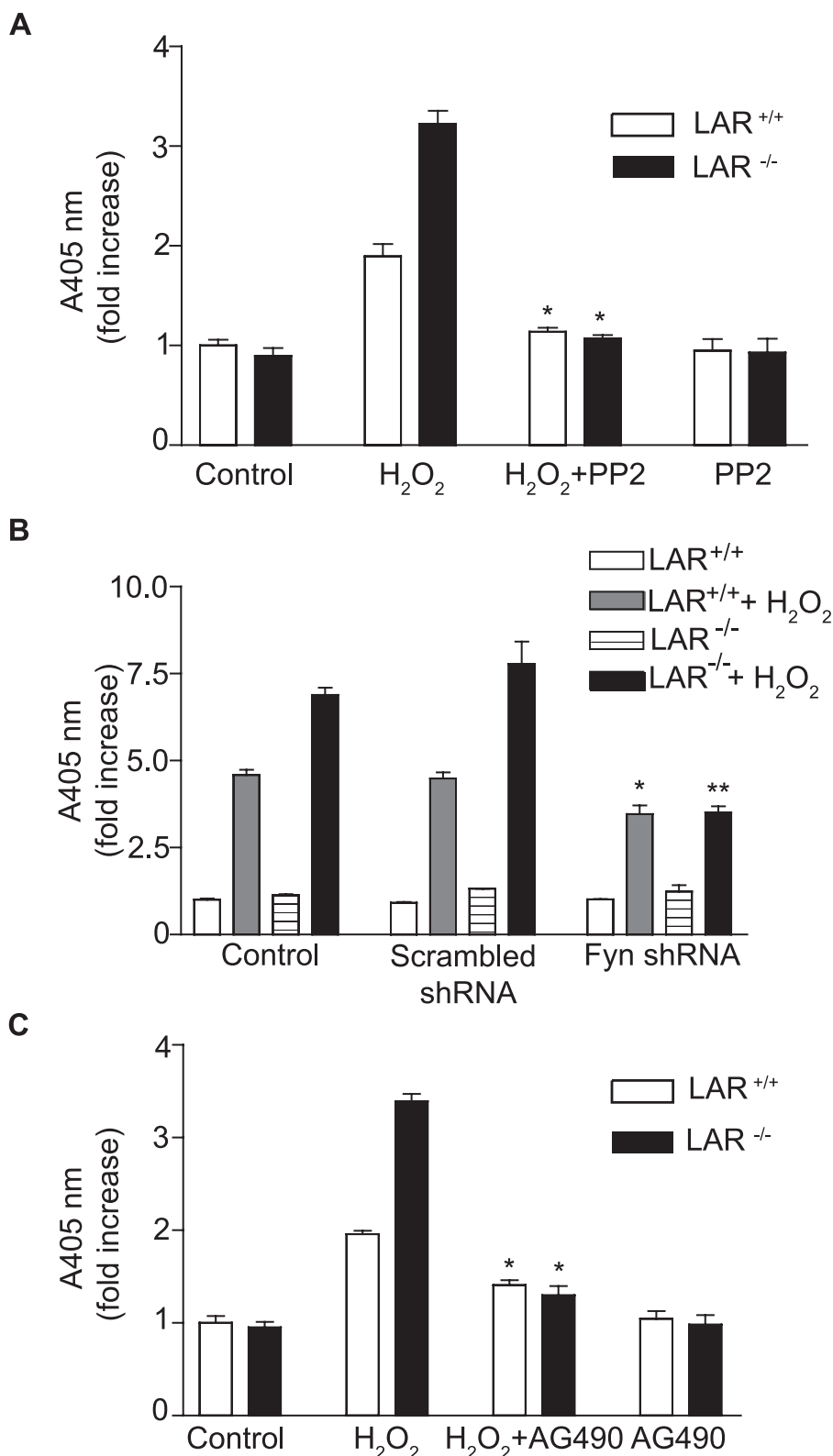
FIGURE 10. **H$_2$O$_2$-induced apoptosis in wild-type and LAR$^{-/-}$ VSMCs is inhibited by PP2, expression of Fyn shRNA, and AG 490.** *A*, growth-arrested VSMCs were pretreated with 1 μM PP2 for 2 h and then treated with 1 mM H$_2$O$_2$ for 16 h. Cell lysates were assayed for histone-associated DNA fragmentation (mean ± S.E., *n* = 3; *, *p* < 0.001 respective H$_2$O$_2$-treated cells). *B*, mock-infected control VSMCs, scrambled shRNA- or Fyn shRNA-expressing LAR$^{+/+}$ and LAR$^{-/-}$ VSMCs clones were growth-arrested and then treated with 1 mM H$_2$O$_2$ for 16 h. Cell lysates were assayed for histone-associated DNA fragmentation (mean ± S.E., *n* = 3; *, *p* < 0.01 *versus* mock-infected H$_2$O$_2$-treated LAR$^{+/+}$ VSMCs; **, *p* < 0.001 *versus* mock-infected H$_2$O$_2$-treated LAR$^{-/-}$ VSMCs). *C*, growth-arrested VSMCs were pretreated with 25 μM AG490 for 16 h and then treated with 1 mM H$_2$O$_2$ for 16 h. Cell lysates were assayed for histone-associated DNA fragmentation (mean ± S.E., *n* = 3; *, *p* < 0.001 respective H$_2$O$_2$-treated cells).

ensures efficient intracellular signal propagation (14, 16, 57). ROS-induced inactivation of PTPs in VSMCs was reported (58, 59), however, the specific role of individual PTP in regulating apoptotic pathways has not yet been investigated. In the present report, we characterize the role of LAR in H$_2$O$_2$-induced apoptosis using VSMCs derived from mice that are deficient in this PTP. Our data indicate that LAR plays an important role in VSMC survival by negatively regulating H$_2$O$_2$-induced Fyn activation and downstream effector pathways of apoptosis.

Our results demonstrate that LAR is inactivated rapidly in VSMCs treated with H$_2$O$_2$. This is consistent with the report of Groen *et al.* (20), which demonstrated that both catalytically active membrane-proximal domain D1 and membrane-distal regulatory domain D2 of LAR are readily oxidized at low H$_2$O$_2$ concentrations, with maximal oxidation at 125–250 μM concentration. However, VSMCs contain several other redox-sensitive PTPs such as SHP-1, PTP1B, and low molecular weight PTP (13), which might become inactive at the H$_2$O$_2$ concentration we used in this study. The use of LAR-deficient VSMCs allowed us to circumvent the confounding effects of other inactivated PTPs following H$_2$O$_2$ treatment and investigate the specific role of LAR in regulating stress-induced apoptotic pathways. Our results show that activation of Fyn in response to H$_2$O$_2$ treatment is transient in wild-type VSMCs, whereas absence of LAR results in sustained activation of this proapoptotic kinase in H$_2$O$_2$-treated cells (Fig. 4).

The critical role of Fyn activation in redox-sensitive mechanisms is evident from the impaired ROS-induced cellular signaling pathways in various Fyn knockout cells (43, 45). Further, caspase activation and DNA fragmentation induced by various proapoptotic stimuli are significantly reduced in embryonic fibroblasts and thymocytes from Fyn knockout mice (60), which
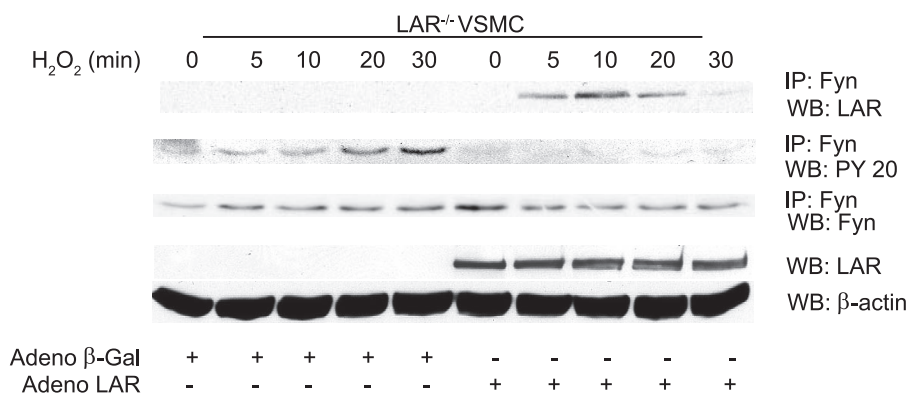
FIGURE 11. **H₂O₂-induced tyrosine phosphorylation of Fyn is attenuated in LAR⁻/⁻ VSMCs overexpressing LAR.** Growth-arrested LAR⁻/⁻ VSMCs, infected with either Adβ-galactosidase or AdLAR, were treated with 1 mM H₂O₂ for the indicated times. Cell lysates were immunoprecipitated with anti-Fyn antibody followed by Western analysis with either anti-LAR antibody, anti-PY20 antibody, or anti-Fyn antibody. Whole cell lysates were analyzed by Western blotting with anti-LAR monoclonal antibody, and the membrane was reprobed with anti-β-actin antibody.

strengthens the idea that Fyn activation is a critical event in stress-induced apoptosis. These observations are in agreement with our data that silencing of Fyn expression by shRNA significantly attenuated H₂O₂-induced downstream signaling pathways (Fig. 8) and apoptosis in both wild-type and LAR knockout VSMCs (Fig. 10).

Regulation of Src-family kinase activity occurs through phosphorylation on two tyrosine residues (48). Autophosphorylation of tyrosine in the activation loop (Tyr-419 in Fyn) increases kinase activity, whereas phosphorylation of tyrosine residue in the C terminus (Tyr-530 in Fyn) inhibits activity through an intramolecular SH2 (Src homology 2)-phosphotyrosine interaction. It has been suggested that dephosphorylation of tyrosine in the C-terminal domain precedes the autophosphorylation of tyrosine in the activation loop for full kinase activity (61). However, Sanguinetti *et al.* (49) demonstrated that, concomitant with autophosphorylation, oxidative stress also increased phosphorylation of the inhibitory site of Fyn, which indicates that activation of Fyn is rapidly followed by inactivation. Activation of Fyn could also be regulated by LAR as this activated PTP is associated with Fyn and dephosphorylates the phosphotyrosine residues in both the kinase domain and C terminus (46). Consistent with these observations, our results demonstrate enhanced association of LAR with activated Fyn in H₂O₂-treated VSMCs (Fig. 5, *A* and *B*) and increased autophosphorylation and sustained activation of Fyn in LAR knockout VSMCs treated with H₂O₂. This occurred despite increased phosphorylation of Tyr-530 in Fyn. Furthermore, absence of LAR impaired mitochondrial membrane potential in VSMCs treated with H₂O₂ and enhanced caspase-3/7 activity and apoptosis (Fig. 2).

Our data indicate increased activation of JAK2 and STAT3 in wild-type VSMCs and significantly enhanced activation of these proteins in LAR knockout VSMCs compared with wild-type cells in response to H₂O₂ treatment. In addition, inhibition of Fyn activity with PP2 pretreatment abrogated H₂O₂-induced JAK2 and STAT3 stimulation in both wild-type and LAR knockout mice. These data are in consonance with the observations that H₂O₂-stimulated JAK2 activity was completely

inhibited in Fyn knockout cells (43) and that Fyn directly interacts with activated JAK2 (62).

The JAK2-specific inhibitor, AG490, not only abrogated H₂O₂-induced stimulation of STAT3 (Fig. 8, *C* and *D*), but also significantly attenuated H₂O₂-induced apoptosis in both wild-type and LAR knockout cells (Fig. 9*B*). These results are in agreement with the observation of Sandberg and Sayeski (50) that activation of JAK2 is essential for H₂O₂-induced apoptosis of VSMCs. They have shown that JAK2 activation leads to induction of proapoptotic Bax expression, impaired mitochondrial membrane integrity, and activation of caspases. Further, AG490 treatment markedly reduced ischemia-induced infarct size and cardiomyocyte apoptosis (63). Although STAT3 activation is usually associated with cell proliferation, strong and prolonged activation of STAT3 induces apoptosis (64, 65), which further supports our conclusions that hyperactivation of the Fyn/JAK2/STAT3 pathway in the absence of LAR induces VSMC apoptosis.

Our data indicate that H₂O₂-induced p38 MAPK activity, which was increased in wild-type VSMCs, was further enhanced in the absence of LAR. PP2 pretreatment abrogated H₂O₂-induced p38 MAPK activity, whereas AG490 had no such inhibitory effect. These data confirm that Fyn is upstream of p38 MAPK activation (51, 52) and that Fyn/JAK2/STAT3 and Fyn/p38 MAPK are two distinct signaling pathways involved in oxidative stress-induced VSMC apoptosis. It is well documented that p38 MAPK plays a critical role in apoptosis induced by several agonists (54, 66, 67). Phosphorylation of Bcl-2 by activated p38 MAPK in mitochondrial compartment leads to cytochrome *c* release and caspase activation, and these processes are absent in p38 MAPK-deficient cells (68).

In conclusion, our results demonstrate that LAR is a redox-sensor and negative regulator of H₂O₂-induced apoptosis in VSMCs. Moreover, our report elucidates Fyn/JAK2/STAT3 and Fyn/p38 MAPK pathways as intracellular mediators of H₂O₂-induced VSMC apoptosis. Our data also suggest tissue/cell-specific effect of LAR as its activation/expression was correlated with increased apoptosis in other tissues (69–71). PTP inhibitor development is an active area of research for the treatment of obesity and diabetes. However, our data cautions on the use of such a strategy, because apoptosis, induced by exacerbated oxidative stress prevalent under such pathophysiological conditions, may profoundly affect many vascular diseases.

REFERENCES

1. Meier, P., Finch, A., and Evan, G. (2000) *Nature* **407,** 796–801
2. Han, D., Haudenschild, C., Hong, M., Tinkle, B., Leon, M., and Liau, G. (1995) *Am. J. Pathol.* **147,** 267–277
3. Geng, Y., and Libby, P. (1995) *Am. J. Pathol.* **147,** 251–266
4. Pollman, M. J., Hall, J. L., and Gibbons, G. H. (1999) *Circ. Res.* **84,** 113–121
5. Bauriedel, G., Hutter, R., Welsch, U., Bach, R., Sievert, H., and Luderitz, B.

(1999) *Cardiovasc. Res.* **41,** 480–488

6. von der Thusen, J. H., van Vlijmen, B. J., Hoeben, R. C., Kockx, M. M., Havekes, L. M., van Berkel, T. J., and Biessen, E. A. (2002) *Circulation* **105,** 2064–2070

7. Clarke, M. C., Figg, N., Maguire, J. J., Davenport, A. P., Goddard, M., Littlewood, T. D., and Bennett, M. R. (2006) *Nat Med.* **12,** 1075–1080

8. Smith, C., Mitchinson, M. J., Aruoma, O. I., and Halliwell, B. (1992) *Biochem. J.* **286,** 901–905

9. Li, P. F., Dietz, R., and von Harsdorf, R. (1997) *FEBS Lett.* **404,** 249–252

10. Sorescu, D., Weiss, D., Lassegue, B., Clempus, R. E., Szocs, K., Sorescu, G. P., Valppu, L., Quinn, M. T., Lambeth, J. D., Vega, J. D., Taylor, W. R., and Griendling, K. K. (2002) *Circulation* **105,** 1429–1435

11. Guo, Z., Mitchell-Raymundo, F., Yang, H., Ikeno, Y., Nelson, J., Diaz, V., Richardson, A., and Reddick, R. (2002) *Mech Ageing Dev.* **123,** 1121–1131

12. Irani, K. (2000) *Circ. Res.* **87,** 179–183

13. Clempus, R. E., and Griendling, K. K. (2006) *Cardiovasc Res.* **71,** 216–225

14. Lee, S. R., Kwon, K. S., Kim, S. R., and Rhee, S. G. (1998) *J. Biol. Chem.* **273,** 15366–15372

15. Meng, T. C., Fukada, T., and Tonks, N. K. (2002) *Mol Cell.* **9,** 387–399

16. Meng, T. C., Buckley, D. A., Galic, S., Tiganis, T., and Tonks, N. K. (2004) *J. Biol. Chem.* **279,** 37716–37725

17. Tang, H., Hao, Q., Rutherford, S. A., Low, B., and Zhao, Z. J. (2005) *J. Biol. Chem.* **280,** 23918–23925

18. Denu, J. M., and Dixon, J. E. (1998) *Curr. Opin. Chem. Biol.* **2,** 633–641

19. Denu, J. M., and Tanner, K. G. (1998) *Biochemistry* **37,** 5633–5642

20. Groen, A., Lemeer, S., van der Wijk, T., Overvoorde, J., Heck, A. J., Ostman, A., Barford, D., Slijper, M., and den Hertog, J. (2005) *J. Biol. Chem.* **280,** 10298–10304

21. Bae, Y. S., Kang, S. W., Seo, M. S., Baines, I. C., Tekle, E., Chock, P. B., and Rhee, S. G. (1997) *J. Biol. Chem.* **272,** 217–221

22. Sundaresan, M., Yu, Z. X., Ferrans, V. J., Irani, K., and Finkel, T. (1995) *Science* **270,** 296–299

23. Hao, Q., Rutherford, S. A., Low, B., and Tang, H. (2006) *Free Radic. Biol. Med.* **41,** 302–310

24. Pulido, R., Serra-Pages, C., Tang, M., and Streuli, M. (1995) *Proc. Natl. Acad. Sci. U. S. A.* **92,** 11686–11690

25. Streuli, M., Krueger, N. X., Ariniello, P. D., Tang, M., Munro, J. M., Blattler, W. A., Adler, D. A., Disteche, C. M., and Saito, H. (1992) *EMBO J.* **11,** 897–907

26. Yu, Q., Lenardo, T., and Weinberg, R. A. (1992) *Oncogene* **7,** 1051–1057

27. Tsujikawa, K., Kawakami, N., Uchino, Y., Ichijo, T., Furukawa, T., Saito, H., and Yamamoto, H. (2001) *Mol. Endocrinol.* **15,** 271–280

28. Longo, F. M., Martignetti, J. A., Le Beau, J. M., Zhang, J. S., Barnes, J. P., and Brosius, J. (1993) *J. Biol. Chem.* **268,** 26503–26511

29. Kulas, D. T., Zhang, W. R., Goldstein, B. J., Furlanetto, R. W., and Mooney, R. A. (1995) *J. Biol. Chem.* **270,** 2435–2438

30. Ahmad, F., and Goldstein, B. J. (1997) *J. Biol. Chem.* **272,** 448–457

31. Ren, J. M., Li, P. M., Zhang, W. R., Sweet, L. J., Cline, G., Shulman, G. I., Livingston, J. N., and Goldstein, B. J. (1998) *Diabetes* **47,** 493–497

32. Niu, X. L., Li, J., Hakim, Z. S., Rojas, M., Runge, M. S., and Madamanchi, N. R. (2007) *J. Biol. Chem.* **282,** 19808–19819

33. Skarnes, W. C., Moss, J. E., Hurtley, S. M., and Beddington, R. S. (1995) *Proc. Natl. Acad. Sci. U. S. A.* **92,** 6592–6596

34. Yang, T., Bernabeu, R., Xie, Y., Zhang, J. S., Massa, S. M., Rempel, H. C., and Longo, F. M. (2003) *J. Neurosci.* **23,** 3353–3363

35. Yeo, T. T., Yang, T., Massa, S. M., Zhang, J. S., Honkaniemi, J., Butcher, L. L., and Longo, F. M. (1997) *J. Neurosci. Res.* **47,** 348–360

36. Moon, S. K., Thompson, L. J., Madamanchi, N., Ballinger, S., Papaconstantinou, J., Horaist, C., Runge, M. S., and Patterson, C. (2001) *Am. J. Physiol.* **280,** H2779–H2788

37. Madamanchi, N. R., Li, S., Patterson, C., and Runge, M. S. (2001) *J. Biol. Chem.* **276,** 18915–18924

38. Channon, K. M., Blazing, M. A., Shetty, G. A., Potts, K. E., and George, S. E. (1996) *Cardiovasc. Res.* **32,** 962–972

39. Kamata, H., Honda, S., Maeda, S., Chang, L., Hirata, H., and Karin, M. (2005) *Cell* **120,** 649–661

40. Lee, C. K., Park, H. J., So, H. H., Kim, H. J., Lee, K. S., Choi, W. S., Lee, H. M., Won, K. J., Yoon, T. J., Park, T. K., and Kim, B. (2006) *Proteomics* **6,** 6455–6475

41. Salvesen, G. S., and Dixit, V. M. (1999) *Proc. Natl. Acad. Sci. U. S. A.* **96,** 10964–10967

42. Sgorbissa, A., Benetti, R., Marzinotto, S., Schneider, C., and Brancolini, C. (1999) *J. Cell Sci.* **112,** 4475–4482

43. Abe, J., and Berk, B. C. (1999) *J. Biol. Chem.* **274,** 21003–21010

44. Yoshizumi, M., Abe, J., Haendeler, J., Huang, Q., and Berk, B. C. (2000) *J. Biol. Chem.* **275,** 11706–11712

45. Abe, J., Okuda, M., Huang, Q., Yoshizumi, M., and Berk, B. C. (2000) *J. Biol. Chem.* **275,** 1739–1748

46. Tsujikawa, K., Ichijo, T., Moriyama, K., Tadotsu, N., Sakamoto, K., Sakane, N., Fukada, S., Furukawa, T., Saito, H., and Yamamoto, H. (2002) *Mol. Cancer Res.* **1,** 155–163

47. Schaapveld, R. Q., Schepens, J. T., Robinson, G. W., Attema, J., Oerlemans, F. T., Fransen, J. A., Streuli, M., Wieringa, B., Hennighausen, L., and Hendriks, W. J. (1997) *Dev. Biol.* **188,** 134–146

48. Mayer, B. J. (1997) *Curr. Biol.* **7,** R295–R298

49. Sanguinetti, A. R., Cao, H., and Corley Mastick, C. (2003) *Biochem. J.* **376,** 159–168

50. Sandberg, E. M., and Sayeski, P. P. (2004) *J. Biol. Chem.* **279,** 34547–34552

51. Samayawardhena, L. A., Hu, J., Stein, P. L., and Craig, A. W. (2006) *Cell Signal.* **18,** 1447–1454

52. Lamalice, L., Houle, F., and Huot, J. (2006) *J. Biol. Chem.* **281,** 34009–34020

53. Diep, Q. N., Touyz, R. M., and Schiffrin, E. L. (2000) *Hypertension* **36,** 851–855

54. Mori-Abe, A., Tsutsumi, S., Takahashi, K., Toya, M., Yoshida, M., Du, B., Kawagoe, J., Nakahara, K., Takahashi, T., Ohmichi, M., and Kurachi, H. (2003) *J. Endocrinol.* **178,** 417–426

55. Valko, M., Leibfritz, D., Moncol, J., Cronin, M. T., Mazur, M., and Telser, J. (2007) *Int. J. Biochem. Cell Biol.* **39,** 44–84

56. Stone, J. R., and Yang, S. (2006) *Antioxid Redox Signal.* **8,** 243–270

57. Chiarugi, P., Fiaschi, T., Taddei, M. L., Talini, D., Giannoni, E., Raugei, G., and Ramponi, G. (2001) *J. Biol. Chem.* **276,** 33478–33487

58. Amiri, F., Venema, V. J., Wang, X., Ju, H., Venema, R. C., and Marrero, M. B. (1999) *J. Biol. Chem.* **274,** 32382–32386

59. Kappert, K., Sparwel, J., Sandin, A., Seiler, A., Siebolts, U., Leppänen, O., Rosenkranz, S., and Ostman, A. (2006) *Arterioscler. Thromb. Vasc. Biol.* **26,** 2644–2651

60. Ricci, J. E., Lang, V., Luciano, F., Belhacene, N., Giordanengo, V., Michel, F., Bismuth, G., and Auberger, P. (2001) *FASEB J.* **15,** 1777–1779

61. Xu, W., Harrison, S. C., and Eck, M. J. (1997) *Nature* **385,** 595–602

62. Uddin, S., Sher, D. A., Alsayed, Y., Pons, S., Colamonici, O. R., Fish, E. N., White, M. F., and Platanias, L. C. (1997) *Biochem. Biophys. Res. Commun.* **235,** 83–88

63. Mascareno, E., El-Shafei, M., Maulik, N., Sato, M., Guo, Y., Das, D. K., and Siddiqui, M. A. (2001) *Circulation* **104,** 325–329

64. Ahmed-Choudhury, J., Williams, K. T., Young, L. S., Adams, D. H., and Afford, S. C. (2006) *Cell Signal.* **18,** 456–488

65. Lu, Y., Fukuyama, S., Yoshida, R., Kobayashi, T., Saeki, K., Shiraishi, H., Yoshimura, A., and Takaesu, G. (2006) *J. Biol. Chem.* **281,** 36683–36690

66. Rosini, P., De Chiara, G., Bonini, P., Lucibello, M., Marcocci, M. E., Garaci, E., Cozzolino, F., and Torcia, M. (2004) *J. Biol. Chem.* **279,** 14016–14023

67. Grethe, S., Ares, M. P., Andersson, T., and Pörn-Ares, M. I. (2004) *Exp. Cell Res.* **298,** 632–642

68. De Chiara, G., Marcocci, M. E., Torcia, M., Lucibello, M., Rosini, P., Bonini, P., Higashimoto, Y., Damonte, G., Armirotti, A., Amodei, S., Palamara, A. T., Russo, T., Garaci, E., and Cozzolino, F. (2006) *J. Biol. Chem.* **281,** 21353–21361

69. Weng, L. P., Yuan, J., and Yu, Q. (1998) *Curr. Biol.* **8,** 247–256

70. Weng, L. P., Wang, X., and Yu, Q. (1999) *Genes Cells* **4,** 185–196

71. Tisi, M. A., Xie, Y., Yeo, T. T., and Longo, F. M. (2000) *J. Neurobiol.* **42,** 477–486